Efficient real-space configuration-interaction method for the simulation of multielectron mixed quantum and classical nonadiabatic molecular dynamics in the condensed phase

Ross E. Larsen and Benjamin J. Schwartz
Department of Chemistry and Biochemistry, University of California, Los Angeles, California 90095-1569

We introduce an efficient configuration interaction (CI) method for the calculation of mixed quantum and classical nonadiabatic molecular dynamics for multiple electrons. For any given realization of the classical degrees of freedom (e.g., a solvent), the method uses a novel real-space quadrature to efficiently compute the Coulomb and exchange interactions between electrons. We also introduce an approximation whereby the classical molecular dynamics is propagated for several time steps on electronic potential energy surfaces generated using only a particularly *important subset* of the CI basis states. By only updating the important-states subset periodically, we achieve significant reductions in the computational cost of solving the multielectron quantum problem. We test the real-space quadrature for the cases of two electrons confined in a cubic box with infinitely repulsive walls and two electrons dissolved in liquid water that occupy a single cavity, so-called hydrated *dielectrons*. We then demonstrate how to perform mixed quantum and classical nonadiabatic dynamics by combining these computational techniques with the mean-field with surface hopping algorithm of Prezhdo and Rossky [J. Chem. Phys. **107**, 825 (1997)]. Finally, we illustrate the practicality of the approach to multielectron nonadiabatic dynamics by examining the nonadiabatic relaxation dynamics of both spin singlet and spin triplet hydrated dielectrons following excitation from the ground to the first excited state. © *2003 American Institute of Physics.*
[DOI: 10.1063/1.1610438]

I. INTRODUCTION

The study of chemical and electronic dynamics in the condensed phase is dominated by simulation techniques in which some degrees of freedom are treated quantum mechanically and the remainder are taken to obey classical mechanics.[1] Such mixed quantum and classical (QM/CM) methods must be used because it is far too computationally expensive to solve the time-dependent Schrödinger equation for every electron and nucleus in a many-body system. Mixed QM/CM methods for electronic dynamics are feasible because the mass difference between electrons and nuclei causes a separation of time scales between electronic and nuclear degrees of freedom, so that electronic motions obey Schrödinger's equation whereas nuclear degrees of freedom propagate according to other rules. The most common approach has been to treat the nuclear dynamics classically, but techniques that include some quantum effects in the nuclear motion, such as second-order quantized Hamiltonian dynamics,[2] semiclassical dynamics,[3] Gaussian wave packet,[4] or quantum-dressed classical mechanics,[5] also have been developed. Although the quantum mechanics of nuclear dynamics is certainly of great interest, here we are concerned with the quantum treatment of the electronic degrees of freedom, so without loss of generality we will consider the nuclei to obey classical mechanics.

The most popular QM/CM dynamics methods can be divided into two main categories: one in which the dynamics is restricted to a single adiabatic electronic state and the other in which the electronic wave function can evolve as a superposition of adiabatic electronic states. Adiabatic methods rely on the Born-Oppenheimer approximation to rigorously separate the electronic motions from the nuclear motions, and the nuclear dynamics is restricted to a single (usually ground state) electronic potential energy surface. Restricting dynamics to the ground state allows the potential energy surface to be calculated for the full many-electron quantum system, which is typically done using density functional theory, as in the Car–Parrinello approach.[6] On the other hand, the restriction to the ground state precludes the option of studying excited-state dynamics, so Born–Oppenheimer-based approaches are incapable of studying photochemical processes or processes such as exciton recombination[7] or curve crossings in molecular reaction dynamics.

In contrast, nonadiabatic methods take into account the fact that the electronic motions cannot be rigorously separated from nuclear motions. Nuclear motions can cause the quantum-mechanical wave function to acquire amplitude on more than one adiabatic potential energy surface. Unfortunately, most implementations of nonadiabatic mixed QM/CM have been limited in the number of quantum mechanical degrees of freedom they treat. This is because nonadiabatic dynamics requires the full many-electron wave function for both the ground and excited states. Thus, condensed phase systems studied with nonadiabatic dynamics, such as solvated electrons,[8–11] proton transfer,[12,13] charge-transfer-to-solvent (CTTS),[14–16] and donor-acceptor electron transfer complexes,[17] typically are simulated with only a single quan-

tum degree of freedom.[18] This restriction to a single quantum degree of freedom is unfortunate because there are several hints that one-electron treatments do not always properly describe the electronic structure of solvated systems. For example, Sheu and Rossky[14] have simulated the nonadiabatic relaxation following CTTS excitation of iodide in water using only a single QM electron that interacted with the iodine core and solvent molecules through pseudopotentials. However, *ab initio* calculations by Bradforth and Jungwirth[19] revealed a completely different structure for the energy levels of aqueous iodide than with the one-electron pseudopotential. In particular, Bradforth and Jungwirth observed only a single bound CTTS excited state, in sharp contrast to the band of six states of mixed *s* and *d* character found in the one-electron calculations. This suggests that the single-electron calculations underestimate the magnitude of the exchange and Coulomb interactions for higher-lying excited states by as much as several eV. Thus, it is unclear exactly what single-electron nonadiabatic dynamics can teach us about the relaxation of real multielectron systems.

To address this gap in existing nonadiabatic simulation methods, in this paper we introduce a new computational method to perform nonadiabatic dynamical simulations of multielectron systems. Our approach to multielectron QM/CM dynamics in the condensed phase is based on calculating adiabatic multielectron wave functions for each nuclear configuration using configuration interaction (CI). In practice, any CI calculation starts with solutions of the single-electron Schrödinger equation, where the numerical solution of Schrödinger's equation requires the choice of some basis in which to expand trial solutions. For gas phase problems involving electron-molecule interactions, it is common to work with bases that explicitly acknowledge the underlying molecular geometry, for example, Slater orbitals or Gaussian basis sets.[20] Condensed-phase problems, in contrast, often lead to electronic states that are not closely associated with just a single molecule. These can be delocalized ''conduction-band-like'' states, or they can be rather localized states, residing mostly ''between'' solvent molecules, so-called solvent-supported states. Thus, to study multielectron systems without biasing the problem, our choice of the one-electron basis must be able to describe both solvent-supported and on-molecule states. The most straightforward choice of basis, and the one we adopt here, is to solve for the electronic wave functions on a grid. This approach avoids bias and is guaranteed to converge as the grid density is increased.

Once the single-electron wave functions have been determined on a grid, the next step of a CI calculation is to evaluate the Coulomb and exchange interactions between antisymmetrized products of the single-electron states. To calculate these electron-electron interactions using grid-based single-electron wave functions, we will introduce a new real-space quadrature that converts the six-dimensional integrations into rapidly convergent double summations over the grid points. Once the electron-electron interactions are determined, the CI calculation gives the *wave functions* for the ground and excited states of the multielectron system, not just the charge densities of these states, allowing matrix elements of observables such as optical transition dipoles to be computed.

With the multielectron eigenstates determined by CI, the solvent dynamics can be propagated using any of a myriad of adiabatic[1,6] or nonadiabatic[1,5,13,21,22] dynamical schemes. Because molecular dynamics simulations require evaluation of multielectron wave functions for thousands of configurations, to make the simulations practical we will also introduce a trick to reduce the computational effort needed for solving the multielectron Schrödinger equation. The trick amounts to determining which single-electron product states contribute appreciably to the full multielectron eigenstates, and then using only this subset of important states in the CI calculations, periodically updating the list of important states.

To test our scheme, we will examine nonadiabatic relaxation dynamics in a two-electron condensed-phase system consisting of two electrons that occupy a single cavity in liquid water, the *hydrated dielectron*. The hydrated dielectron serves as a useful test of our real-space CI method because it is closely related to the well-studied case of the single hydrated electron.[8–11,23–26] The hydrated dielectron is also of interest because it contains *only* electron–solvent interactions, thus allowing for a detailed study of the interplay between electron-electron and electron–solvent interactions without complications that might arise from intramolecular electronic structure. Thus, we will investigate a model system that maximizes the ability of the *solvent* to modulate the two-electron wave function, subject only to those constraints imposed by the electron-electron interaction and spin statistics.

In the results presented below for nonadiabatic relaxation by the hydrated dielectron, we will use Prezhdo and Rossky's mean-field with surface hopping (MF/SH) approach[21] for nonadiabatic dynamics. This method lets the classical degrees of freedom evolve according to Ehrenfest's theorem, but also incorporates decoherence and nonadiabatic effects by letting the wave function evolve discontinuously, either by mean-field rescaling or via surface hops (electronic transitions between different adiabatic electronic states). We have chosen this nonadiabatic dynamics algorithm because of the ease with which it can be implemented for QM problems of any dimensionality.

The rest of this paper is organized as follows. In Sec. II we briefly review the CI method and introduce the aforementioned real-space quadrature for evaluation of the Coulomb and exchange integrals. We then test this quadrature for the case of two electrons confined to a cubic box and examine the convergence of our real-space CI method for a hydrated dielectron in a single configuration of liquid water. Section III shows how to use the CI method for molecular dynamics and introduces the idea of saving computational effort by using only an ''important'' subset of the two-electron product basis for the dynamics, with occasional updates of the important-states subset. In Sec. IV we apply our new methods to the condensed-phase dynamics problem of the dielectron in liquid water, showing examples of nonadiabatic MF/SH dynamics for both singlet- and triplet-paired dielectrons. For completeness, we include an Appendix with a dis-

cussion of the details of how to implement the MF/SH algorithm with CI wave functions. We conclude in Sec. V with a discussion of the full multielectron, nonadiabatic, mixed QM/CM method and some thoughts on future directions.

II. MANY-ELECTRON WAVE FUNCTIONS USING REAL-SPACE CONFIGURATION INTERACTION

A. Review of the configuration-interaction method

The CI method (in principle) allows the exact construction of the eigenstates of a system of interacting electrons. This technique is well known,[27] but in order to fix our notation for the rest of this paper, we first briefly review the method.

Configuration interaction calculations solve Schrödinger's equation for M electrons by first finding approximate single-electron eigenstates and then constructing the interaction potential in a basis of appropriately antisymmetrized product states. The so-called "singles and doubles" prescription reduces the problem to just two electrons, with the "noninteracting" basis states determined self-consistently so as to take into account the interactions with the remaining $M-2$ electrons. For only two electrons, the exact one-electron states are used to construct the basis (i.e., no self-consistent calculation is needed) and the single and double excitations form a complete basis. Thus, for the two-electron problem, "CI with singles and doubles" is equivalent to full, multireference CI.

Consider the Hamiltonian for two interacting electrons,

$$\hat{H}_{12} = \hat{H}_1 + \hat{H}_2 + \hat{V}_{12}, \qquad (1)$$

where the subscripts indicate which electron(s) the operator acts upon.[28] The operators $\hat{H}_1$ and $\hat{H}_2$ consist of the kinetic energy and the external potential energy (e.g., from a solvent) operators for each electron, and the interaction between the electrons is a Coulomb repulsion,[29]

$$\langle \mathbf{r}_1', \mathbf{r}_2' | \hat{V}_{12} | \mathbf{r}_1, \mathbf{r}_2 \rangle = \left(\frac{e^2}{r_{12}} \right) \delta(\mathbf{r}_1' - \mathbf{r}_1) \delta(\mathbf{r}_2' - \mathbf{r}_2), \qquad (2)$$

where $r_{12} = |\mathbf{r}_1 - \mathbf{r}_2|$. Let us denote the single-electron eigenenergies and eigenstates of $\hat{H}_1$ and $\hat{H}_2$ by ϵ_n and $|n\rangle$ [or $\langle \mathbf{r} | n \rangle \equiv \psi_n(\mathbf{r})$], respectively. A two-electron state can be expanded in terms of appropriately antisymmetrized products of single-electron states (in a direct-product Hilbert space),

$$|nm\rangle_\pm = (|n\rangle|m\rangle \pm |m\rangle|n\rangle)/\sqrt{2} \quad (m > n) \qquad (3)$$

and

$$|nn\rangle_+ = |n\rangle|n\rangle. \qquad (4)$$

Here the plus sign is used for spin-singlet pairs and the minus sign when the spins are triplet paired, and for notational simplicity, we have supressed the relevent spinor products. Note that the use of N one-electron eigenstates gives $N(N+1)/2$ spin-singlet or $N(N-1)/2$ spin-triplet product basis states; by convention we construct the basis using only $m \geq n$.

The remaining steps in the CI calculation proceed as follows. Once we have found N single-electron states, we write the two-electron eigenstates as linear combinations of product basis states,

$$|\Psi\rangle_\pm = \sum_{n,m} c_{nm} |nm\rangle_\pm . \qquad (5)$$

The time-independent Schrödinger equation implies that

$$\sum_{nm} c_{nm} (\hat{H}_1 + \hat{H}_2 + \hat{V}_{12}) |nm\rangle_\pm = E \sum_{nm} c_{nm} |nm\rangle_\pm , \qquad (6)$$

from which it is easily seen that the eigenvalues $\{E_i\}$ and expansion coefficients $\{c_{nm}^i\}$ are given by the eigenvalues and eigenvectors of the $N(N\pm 1)/2 \times N(N\pm 1)/2$ Hamiltonian matrix $(\hat{H}_1 + \hat{H}_2 + \hat{V}_{12})$ (for notational convenience we have supressed the $\pm$ index on the c_{nm}).

The antisymmetrized product states $|nm\rangle_\pm$ are eigenstates of $\hat{H}_1 + \hat{H}_2$,

$$(\hat{H}_1 + \hat{H}_2)|nm\rangle_\pm = (\epsilon_n + \epsilon_m)|nm\rangle_\pm , \qquad (7)$$

so that $\hat{H}_1 + \hat{H}_2$ is diagonal in this basis. The interaction, on the other hand, is not diagonal, and its matrix elements are

$$\begin{aligned} {}_\pm\langle n'm'|\hat{V}_{12}|nm\rangle_\pm = \int d\mathbf{r}_1 \int d\mathbf{r}_2 \left(\frac{e^2}{r_{12}} \right) \\ \times \{ \psi_{n'}^*(\mathbf{r}_1) \psi_n(\mathbf{r}_1) \psi_{m'}^*(\mathbf{r}_2) \psi_m(\mathbf{r}_2) \\ \pm \psi_{m'}^*(\mathbf{r}_1) \psi_n(\mathbf{r}_1) \psi_{n'}^*(\mathbf{r}_2) \psi_m(\mathbf{r}_2) \}, \quad (8) \end{aligned}$$

$$\begin{aligned} {}_+\langle n'n'|\hat{V}_{12}|nm\rangle_+ = \sqrt{2} \int d\mathbf{r}_1 \int d\mathbf{r}_2 \left(\frac{e^2}{r_{12}} \right) \\ \times \{ \psi_{n'}^*(\mathbf{r}_1) \psi_n(\mathbf{r}_1) \psi_{n'}^*(\mathbf{r}_2) \psi_m(\mathbf{r}_2) \}, \quad (9) \end{aligned}$$

and

$$\begin{aligned} {}_+\langle n'n'|\hat{V}_{12}|nn\rangle_+ = \int d\mathbf{r}_1 \int d\mathbf{r}_2 \left(\frac{e^2}{r_{12}} \right) \\ \times \{ \psi_{n'}^*(\mathbf{r}_1) \psi_n(\mathbf{r}_1) \psi_{n'}^*(\mathbf{r}_2) \psi_n(\mathbf{r}_2) \}. \quad (10) \end{aligned}$$

The first term in Eq. (8) is called the Coulomb integral, while the second $(\pm)$ term is called the exchange integral; by convention, we take Eqs. (9) and (10) to contribute half of their value to the Coulomb energy and the other half to the exchange energy (this is consistent with the division typically made in, e.g., Hartree–Fock calculations[20]).

Equations (6)–(10) must be solved to determine the two-electron eigenstates. The numerical bottleneck in any CI calculation lies in evaluating the Coulomb and exchange integrals of Eqs. (8)–(10), and it is this problem to which we turn our attention in the next subsection.

B. Real-space quadrature for the Coulomb and exchange integrals

As we have already pointed out, it is often desirable for numerical solutions of the single-electron wave functions to be defined only at discrete grid points; this is the case for the block-Lanczos method we use below in Sec. IV in solving

the example problem of a dielectron in liquid water. The integrals we need to evaluate in Eqs. (8)–(10) assume, however, that the wave functions are defined everywhere in space, not just at the $N_c \equiv N_g^3$ points on a cubic grid. We must therefore develop a scheme that converts grid-based wave functions into continuous functions suitable for insertion into the above integrands.

One such approach would be to expand the wave function in a Fourier or other series, but in a disordered system such expansions can actually increase the computational expense beyond that of a direct, real-space approach. To make this point clear, suppose that each one-electron state were expanded in a series,

$$\psi_n(\mathbf{r}) = \sum_{i=1}^{N_c} a_n^i f_i(\mathbf{r}),$$

turning each Coulomb or exchange integral in Eqs. (8)–(10) into a fourfold summation over expansion coefficents, with a summand that could be nonzero for as many as N_c^4 terms. In a disordered system such as a liquid, we would expect such an expansion to contain so many terms that the fourfold summation would be highly inefficient. Note that the fourfold summation arises in this CI calculation because we expand the two-electron wave functions in a product-state basis. As an alternative, we could work directly with the product states,

$$\psi_n(\mathbf{r})\psi_m^\star(\mathbf{r}) = \sum_{i=1}^{N_c} A_{nm}^i f_i(\mathbf{r}).$$

Working in terms of products of single-electron wave functions is akin to forming charge densities, so such a method would be similar in computational cost to the Hartree term in density functional calculations. Indeed, if the expansion coefficients A_{nm} are known from previous steps in the calculation, this alternate expansion reduces the transformed two-electron integrations from order N_c^4 to order N_c^2—the same cost as the real-space integration. If, on the other hand, the coefficients must be computed separately, the additional computations (of order N_c^2 in general or $N_c \log_2 N_c$ for a fast Fourier transform) make the transformed integration scheme more expensive than in real space. Clearly, working with such expansions makes sense if only a small subset of terms in the expansion contributes to each single-electron state. The wave functions typical of electrons in disordered media, however, cannot be represented by just a few plane waves or other orthogonal polynomials. For such disordered systems, we anticipate that calculating the six-dimensional Coulomb and exchange integrals directly in real space, an order N_c^2 operation, will be computationally most efficient with CI, provided that we can perform the real-space integrations with accuracy comparable to that of Fourier methods. It is to this problem that we now turn our attention.

To compute the Coulomb and exchange integrals in real space with grid-based single-electron wave functions, the wave functions need to be defined everywhere in space. It turns out that a low-order, finite-element approximation suffices and leads directly to a simple quadrature for evaluating the Coulomb and exchange integrals, Eqs. (8)–(10). Our finite-element approach assumes that the one-electron wave function can be represented by a power series inside a cube of side a around each grid point $\mathbf{r}_i$ (the grid also has spacing a),

$$\widetilde{\psi}_n(\mathbf{r}) = [\psi_n(\mathbf{r}_i) + (\mathbf{r} - \mathbf{r}_i) \cdot \nabla \psi_n(\mathbf{r}_i) + \cdots]/W, \tag{11}$$

where the factor W is there to preserve normalization of the new (piecewise continuous) wave function upon converting the normalization sum, $\Sigma_i |\psi_n(\mathbf{r}_i)|^2 = 1$, into an integral over the simulation volume. We have found that the lowest-order, or piecewise-constant, expansion yields sufficient accuracy for our purposes, so this rescaling amounts to dividing the grid-based wave function by the square root of the cube's volume, $\widetilde{\psi}_n(\mathbf{r}) = \psi_n(\mathbf{r}_i)/\sqrt{a^3}$, in each cube.

Taking the wave functions to be piecewise constant immediately reduces the Coulomb and exchange integrals to a double sum over grid points (an order N_c^2 quadrature) of the general form

$$I_{abcd} = \int d\mathbf{r}_1 \int d\mathbf{r}_2 \left(\frac{e^2}{r_{12}}\right) \widetilde{\psi}_a^*(\mathbf{r}_1) \widetilde{\psi}_b(\mathbf{r}_1) \widetilde{\psi}_c^\star(\mathbf{r}_2) \widetilde{\psi}_d(\mathbf{r}_2)$$

$$= e^2 \sum_{i=1}^{N_c} \widetilde{\psi}_a^*(\mathbf{r}_i) \widetilde{\psi}_b(\mathbf{r}_i) \sum_{j=1}^{N_c} \widetilde{\psi}_c^\star(\mathbf{r}_j) \widetilde{\psi}_d(\mathbf{r}_j)$$

$$\times \int_{Cube\ i} d\mathbf{r}_i \int_{Cube\ j} d\mathbf{r}_j \frac{1}{r_{ij}}. \tag{12}$$

This expression can be rewritten directly in terms of the *unrescaled* (grid-based) wave functions

$$I_{abcd} = \frac{e^2}{a} \sum_{i=1}^{N_c} \psi_a^\star(\mathbf{r}_i) \psi_b(\mathbf{r}_i) \sum_{j=1}^{N_c} \psi_c^\star(\mathbf{r}_j) \psi_d(\mathbf{r}_j) \phi_{ij}, \tag{13}$$

where

$$\phi_{ij} = \int_0 d\mathbf{r} \int_{|i-j|} d\mathbf{r}' \frac{1}{|\mathbf{r} - \mathbf{r}'|} \tag{14}$$

is the electrostatic potential energy between uniformly charged unit cubes, one centered at the origin, the other centered at grid point $i-j$, in a grid of unit spacing. Because ϕ_{ij} is independent of any physical parameters in the system, we need only tabulate it *once* for any given N_g and can thereafter use the table for any CI calculation.

The question of how to efficiently compute integrals having the form of our ϕ_{ij} has been addressed in a recent paper by Finocchiaro, Pellegrini, and Bientinesi,[30] who showed how to convert six-dimensional integrals containing a $1/r_{12}$ kernel into two-dimensional integrals in which the Coulomb singularity is already integrated out; the remaining two integrations (which must be evaluated numerically) converge rapidly. We have not found it necessary to use this mapping for our Eq. (14) because the six-dimensional integrals also can be calculated to a relative accuracy of $\mathcal{O}(10^{-8})$ or better using the numerical integration routines in Mathematica. These integrations only need to be performed once for each of the $N_g(N_g+1)(N_g+2)/6$ pairs of cubes that have distinct values of ϕ_{ij}.[31] For $N_g = 16$, tabulating ϕ_{ij}

TABLE I. Interaction energies (hartrees) for two electrons confined to an infinite cubic box 1 a.u. on a side. The energies reported are the sum of Coulomb and exchange integrals $[\pm\langle n_x n_y n_z n'_x n'_y n'_z \times |(e^2/r_{12})|n_x n_y n_z n'_x n'_y n'_z\rangle_\pm]$ and the error is computed relative to the results of Alavi (Ref. 33). Note that Alavi has tabulated more integrals than we report here; we find the same rate of convergence and level of error for all reported integrals. Because the Coulomb interaction is scale invariant, the result for other box sizes L can be found by dividing the tabulated results by L in a.u.

N_{grid}	$(n_x n_y n_z , n'_x n'_y n'_z)$	Singlet (relative error)[a]	Triplet (relative error)[a]
8	(111,111)	2.9932 (1.79%)	⋯
16	(111,111)	3.0341 (0.45%)	⋯
24	(111,111)	3.0417 (0.20%)	⋯
32	(111,111)	3.0444 (0.12%)	⋯
8	(111,112)	3.2469 (2.20%)	2.1257 (0.13%)
16	(111,112)	3.3016 (0.55%)	2.1282 (0.009%)
24	(111,112)	3.3117 (0.24%)	2.1284 (0[b])
32	(111,112)	3.3253 (0.16%)	⋯
8	(111,123)	2.5448 (1.90%)	2.2969 (0.27%)
16	(111,123)	2.5818 (0.47%)	2.3028 (0.013%)
24	(111,123)	2.5887 (0.20%)	2.3031 (0[b])
32	(111,123)	2.5910 (0.12%)	⋯

[a]The error is calculated relative to the values reported in Ref. 33.
[b]Identical to the five figures reported in Ref. 33.

took just a few hours on a midrange PC; larger grid sizes can be easily accomodated by noting that for well-separated cubes, ϕ_{ij} rapidly approaches $1/r_{ij}$.[32]

C. Test of the real-space quadrature: Two electrons in a cubic box

Perhaps the simplest example of an interacting-electron system is the case of two electrons in a box bounded by infinite walls. This system recently has been studied in detail by Alavi,[33] who obtained exact solutions for this system via CI using a very efficient hybrid real-space/Fourier-space quadrature to evaluate the Coulomb and exchange integrals, Eqs. (8)–(10). As a test of the accuracy of our (six-dimensional) real-space technique, we have compared the sum of the Coulomb and exchange integrals for the case of two electrons in a cubic box computed using Eq. (13) to the values tabulated by Alavi. The one-electron states $[\psi_{n_x,n_y,n_z}(\mathbf{r})\propto \sin(n_x\pi x/L)\sin(n_y\pi y/L)\sin(n_z\pi z/L)$, where L is the box length] were generated analytically on the grid; product basis states were formed as described in Sec. II A. The results are summarized in Table I for a cube 1 a.u. on a side. Although our real-space method is less computationally efficient than the hybrid real-space/Fourier-space method introduced by Alavi, we see that our method converges rapidly with the number of grid points and gives similar accuracy.

The more rapid convergence of Alavi's hybrid Fourier method requires tuning of a length-scale parameter associated with dividing the Coulomb and exchange integrals into real-space and Fourier-space parts. It is interesting to note that for the (111,112) singlet case, Alavi also has computed the sum of Coulomb and exchange integrals using a direct real-space quadrature that still contains the singular $1/r_{12}$ term in the integrand. This so-called "brute force" approach has an error of roughly 2% with $N_g = 16$, as compared to our

TABLE II. Singlet dielectron energies (eV) in a representative equilibrated water configuration as a function of the number of single-electron states used in the CI calculation, with $N_g = 16$. The number of states in the symmetrized product basis is $N_{states}(N_{states}+1)/2$.

N_{states}	E_1	E_2	E_3	E_4
4	−5.90	−3.10	−2.62	−2.21
8	−6.30	−3.79	−3.37	−3.24
10	−6.53	−3.99	−3.45	−3.38
12	−6.54	−4.26	−3.59	−3.46
15	−6.55	−4.29	−3.73	−3.61

error of only 0.55%. We believe that our real-space quadrature, Eq. (13), converges more rapidly than Alavi's brute-force version because we preintegrated over the singular kernel when we tabulated ϕ_{ij}. Although Alavi's hybrid real-space/Fourier-space approach is much more efficient than our quadrature for this particular example, Alavi's hybrid method is limited to problems for which the single-electron basis states can be represented by just a few Fourier components. The extra efficiency could not be realized for disordered condensed-phase systems because, as we discussed in Sec. II B, such systems would not have single-electron basis states made up of just a few Fourier components. We believe that our real-space quadrature gives the best combination of efficiency and generality for calculating electron-electron interactions with grid-based wave functions in disordered systems.

D. Application to the condensed phase: The dielectron in water

We now apply our method to the hydrated dielectron. This dielectron system is similar to the two-electrons-in-a-box case discussed above in that the electrons are confined to a cavity by the repulsive water-electron pseudopotential,[24] but it is different in that solvation provides an attractive well in addition to the repulsive confining potential, and that the cavity size and shape will fluctuate in time. The single-electron wave functions for this system cannot in general be represented by just a few Fourier components, so this problem is just the sort for which our real-space quadrature, Eq. (13), was designed. In our calculations, the electron-water interaction is taken to be the pseudopotential of Schnitker and Rossky,[24] allowing us to make a direct comparison of the properties of the dielectron with the large body of literature on the single electron generated using this pseudopotential.[11,23,25] Details of the model and the numerical methods are given in Sec. IV A.

Tables II and III show the lowest four two-electron energies for bound spin-singlet and spin-triplet dielectrons, respectively, as functions of the number of single-electron states used to form the CI basis. In each case, the energetics are calculated using a single equilibrated water configuration taken from an equilibrium molecular dynamics simulation run on either the singlet or triplet ground-state surface, as described in Sec. IV B. In both cases, it seems that at least 12 single-electron states must be used for the basis to achieve energies accurate to better than a few $k_B T$. However, the computational cost of the Coulomb and exchange energies

TABLE III. Triplet dielectron energies (eV) in a representative equilibrated water configuration as a function of the number of single-electron states used in the CI calculation, with $N_g = 16$. The number of states in the antisymmetrized product basis is $N_{states}(N_{states}-1)/2$.

N_{states}	E_1	E_2	E_3	E_4
4	-4.16	-2.04	-1.89	-0.78
8	-4.47	-2.34	-2.19	-1.84
10	-4.50	-2.44	-2.25	-1.87
12	-4.50	-2.49	-2.28	-1.90
15	-4.51	-2.50	-2.36	-1.91

scales as N_{states}^4, so it is desirable to use as small an N_{states} as possible. We have found that a choice of $N_{states} = 10$ is satisfactory for our molecular dynamics because errors associated with integrating the equations of motion produce energy fluctuations larger than the error made by keeping only 10 states; thus, as we discuss in more detail in Sec. IV, $N_{states} = 10$ is large enough to adequately conserve the total energy in our MD runs.

III. MAKING MIXED QUANTUM AND CLASSICAL DYNAMICS WITH CI PRACTICAL: THE "IMPORTANT" STATES APPROXIMATION

Although we have established that the real-space CI method can be used to determine eigenstates for any one realization of the single-electron potential, there is still some work to be done before the CI prescription can be used in molecular dynamics (MD) simulations. This is because in MD simulations, the electronic eigenstates and the force that the electrons exert on the classical degrees of freedom need to be calculated at every time step—leading to thousands of nontrivial CI calculations even for simulations of modest length. The slowest step in our grid-based CI implementation turns out to be computing the Coulomb and exchange integrals, Eqs. (8)–(10), between all pairs of product basis states. For example, with 10 single-electron states (which gives 55 product basis states), we must compute $54 \times 55/2 = 1485$ distinct six-dimensional Coulomb and exchange integrals; for a 16^3 grid, this calculation took of order 5 min on an AMD Athlon 1.7 GHz PC. To make dynamics practical we must therefore find a way to reduce the number of matrix elements of $\hat{V}_{12}$ that have to be computed at every time step.

Our solution is to make use of the fact that most of the product basis states contribute very little to any of the lower-lying two-electron eigenstates. We make this idea quantitative by ordering the product basis states $|nm\rangle_\pm$ by the amount they contribute to a given eigenstate, c_{nm}^i [Eq. (5)], and seeing how many basis states, N_{imp}, are "important"— that is, how many are needed for the sum of their contributions, $\sum_{nm}^{N_{imp}} |c_{nm}^i|^2$, to be greater than some fraction f_{imp}. For example, the aqueous singlet dielectron typically needs only 15 product basis states to add up to 99.9% of the ground-state wave function ($f_{imp} = 0.999$). The ground-state energy computed in this 15 basis-state subspace differs from the full 55 basis state (i.e., all two-electron configurations with 10 single-electron eigenstates) energy by only $\sim 0.1\%$. To achieve 99.95% accuracy ($f_{imp} = 0.9995$), 19 product-

basis states must be kept on average, leading to energies within 0.06% of the full 55 basis-state result. Keeping only 19 of the 55 basis states results in an eightfold reduction in the number of CI matrix elements that need to be calculated.

For molecular dynamics, the reductions in computational effort discussed above will hold only as long as the important subspace remains unchanged. Our goal is to run dynamics using only the important subsbace for some time τ_{update} before needing to recalculate the *full* two-electron CI matrix. This idea of explicitly using only a subset of basis states and periodically updating the subset is reminiscent of the neighbor lists used in classical molecular dynamics simulations.[34] The fraction of the eigenvector that needs to be kept, f_{imp}, and the time between updates, τ_{update}, must be determined empirically on a case by case basis. We have chosen f_{imp} and τ_{update} by requiring that molecular dynamics conserve energy.

Insight into how to choose the parameters f_{imp} and τ_{update} can be gained by examining the amount of computational effort saved with this prescription. On average, for a given value of f_{imp}, the important basis uses only N_{imp} product states out of the N_{tot} available. Therefore, for each time step between updates, we perform $(N_{imp}/N_{tot})^2$ as many computations as we would with the full basis. Mathematically, given a molecular dynamics time step Δt and the time between updates, τ_{update}, we perform only a fraction

$$\eta(\Delta t; N_{imp}, \tau_{update}) = \left(\frac{N_{imp}}{N_{tot}}\right)^2 \left(1 - \frac{\Delta t}{\tau_{update}}\right) + \left(\frac{\Delta t}{\tau_{update}}\right) \quad (15)$$

as many computations as without the important-states approximation. The first term in Eq. (15) gives the computational cost of the CI calculation for times between updates, and the second term gives the cost associated with periodically recomputing the full CI matrix. Equation (15) shows that a balance must be struck between keeping as few states as possible but having to update more frequently and calculating a larger number of states but updating the important basis less often.

The above discussion implicitly assumes that only a single two-electron state is of interest at any given instant. However, any calculation that allows nonadiabatic dynamics requires knowledge of more than just the occupied state—for surface hopping or mean-field dynamics, we also need to know about *unoccupied* states—so we need to generalize the idea of the important-states subspace. When the important basis states have been selected to accurately represent only a single two-electron eigenstate, the other two-electron eigenstates formed from the subspace-only Hamiltonian will not necessarily be related to any of the two-electron eigenstates of the full Hamiltonian. We therefore also need to keep in our subspace the product basis states that are important for *each* two-electron eigenstate of interest. For the aqueous dielectron, for instance, representing each of the lowest four two-electron eigenstates to 99.95% accuracy requires 46 of the 55 product basis states; for this case, the important-states approximation gives very little computational benefit. However, accurate dynamics does not necessarily require such precision for *every* two-electron eigenstate. It turns out that we only need high accuracy for two-electron eigenstates that

have appreciable amplitude; weakly populated two-electron states do not need to be as well represented to maintain energy conservation in the molecular dynamics. We have found that in MF/SH simulations of the aqueous dielectron, it suffices to represent the unoccupied eigenstates at $f_{imp} = 99\%$ to maintain energy conservation in the molecular dynamics, as described below in Sec. IV A. This prescription requires on average just 36 important-basis states to describe the lowest six singlet eigenstates (six being all that are needed for the nonadiabatic runs described below). For the spin-triplet case, we find that only 33 of 45 basis states are needed to get the lowest six eigenstates (needed for the nonadiabatic run below) to an accuracy of $f_{imp} = 0.9995$ for the ground eigenstate and $f_{imp} = 0.99$ for the other eigenstates.

IV. APPLICATION: DYNAMICS OF THE AQUEOUS DIELECTRON

In this section, we will demonstrate the ability of our real-space CI method to calculate the nonadiabatic relaxation dynamics for the two-electron condensed-phase case of the hydrated dielectron. Although there has been disagreement about whether the hydrated dielectron has been directly observed in flash photolysis experiments,[35] Schmidt and Bartels have argued[36] that the lack of an ionic strength effect in the recombination of *single* hydrated electrons, $e_{aq}^{-} + e_{aq}^{-} \rightarrow 2OH^{-} + H_2$, implies that paired electrons should be stable. Semicontinuum dielectric calculations also suggest that the singlet hydrated dielectron should exist.[37] In addition, the ground state of the dielectron has been studied in water clusters by Kaukonen *et al.*[38] using spin density functional theory. In order to accelerate the statistical sampling, of electron-water configurations, these workers set the mass of oxygen equal to that of hydrogen; thus, the trajectories in Ref. 38 do not contain dynamical information and serve only to sample phase space. Furthermore, because the system was forced to run on the absolute ground state, the dielectron occasionally switched back and forth between singlet and triplet spin states. This switching is unexpected because nonadiabatic effects cannot produce intersystem crossings from one spin state to another. Spin-singlet and spin-triplet states mix only in the presence of magnetic fields,[29] so the intersystem crossing observed by Kaukonen *et al.* must be an artifact of restricting the dynamics to the global ground state. Stable dielectrons in ammonia have also been predicted by Deng, Martyna, and Klein, who used spin density functional theory combined with Car-Parrinello simulation[39] to study metal-ammonia solutions for metal concentrations that allow the formation of dielectrons.

A. Model and computational details

Our simulation of the hydrated dielectron consists of 200 classical water molecules and two QM electrons. We model the water using SPC-flex potentials[40] and propagate the classical trajectories using the Verlet algorithm[34] with a time step of $\Delta t = 0.5$ fs. As mentioned in Sec. II D, we describe the water-electron interaction using the pseudopotential of Schnitker and Rossky,[24] and calculate the force of the electrons on the water using the Hellmann-Feynman formula (see the Appendix). The constant N, V, E simulations had a temperature of ~ 300 K and took place in a box 18.17 Å on a side, giving a density of 0.997 g/cm^3. The single-electron eigenstates are calculated using an iterative block-Lanczos procedure described in detail elsewhere.[8] For the dielectron in water, a grid size of $N_g = 16$ is the minimum necessary to adequately solve the discretized Schrödinger equation with the iterative block-Lanczos procedure, and we use this grid size for all dielectron calculations reported in this paper.

Because CI is just a general method for finding adiabatic multielectron eigenstates, we can in principle use any nonadiabatic molecular dynamics algorithm to model dielectronic relaxation. Since the two-electron CI calculation is the most computationally expensive step, we restrict ourselves to nonadiabatic methods that rely only on local information about the two-electron wave function. We therefore do not consider methods that require self-consistent or nonlocal calculations, such as the stationary phase surface hopping algorithm.[8,41] From the remaining local nonadiabatic methods, we choose to use Prezhdo and Rossky's MF/SH method,[21] which combines mean-field (Ehrenfest) dynamics[42] (including occasional collapses of the wave function to take into account decoherence) with Tully's fewest-switches surface hopping [also known as molecular dynamics with quantum transitions (MDQT)].[13,22] Both MDQT and MF/SH are attractive choices for many-electron nonadiabatic dynamics because in these methods calculation of the Hellmann-Feynman (HF) forces and the nonadiabatic coupling scale linearly with the number of electrons. We choose MF/SH instead of MDQT because MF/SH does not require a swarm of trajectories from each classical initial condition—thus, within the stochastic approximations described in the Appendix, every MF/SH trajectory is physically meaningful. The details of MF/SH, along with explicit formulas for the nonadiabatic coupling and hopping probabilities for the multielectron case, are given in the Appendix. The time-dependent Schrödinger equation was propagated between molecular-dynamics time steps using a fourth-order Runge–Kutta integrator, with a time step $\delta t = \Delta t / 500$ and a linear interpolation between the two-electron eigenenergies at times t and $t + \Delta t$. The mean-field consistency criteria were taken to be violated when the momentum condition [Eq. (A5)] is larger than 0.1 and when the position condition [Eq. (A6)] becomes larger than the Bohr radius a_0. In the runs reported here, mean-field rescaling occurred only from violations of the momentum condition.

As we discussed in Secs. II D and III, in order to make molecular dynamics with CI wave functions practical, we must set three parameters; the number of one-electron states used for the product basis, N_{states}: the fraction of the eigenvectors kept when determining the important states, f_{imp}; and the time between updates of the important states, τ_{update}. These parameters must be chosen so as to minimize computational cost while maintaining correct dynamics; we gauge the correctness of the dynamics by requiring the total energy of the mixed QM/CM system to be conserved.[43]

The first parameter to be set is the number of single-electron states used to construct the product basis, N_{states}. We determined this parameter by running ground-state, spin-singlet dynamics and constructing the *full* CI matrix at *every*

J. Chem. Phys., Vol. 119, No. 15, 15 October 2003

Nonadiabatic molecular dynamics   7679

TABLE IV. Efficiency gains for different "important-states" parameters for spin-singlet hydrated dielectrons. The results were calculated using Eq. (15), with $N_{states}=10$ used to construct the product basis and τ_{update} chosen to be as large as possible while maintaining energy conservation. The third and fourth columns give the result when only the ground state is used to generate the important-states basis. The right-most column estimates the computational efficiency for nonadiabatic dynamics with a time step $\Delta t = 0.5$ fs, keeping accuracy for the lowest six two-electron energies. The total number of important states, N_{imp}, was the average found from three representative water configurations, with f_{imp} for the first excited state given in the table and with $f_{imp}=0.99$ for the remaining five states.

f_{imp}	τ_{update} (fs)	$\eta(\Delta t = 1.0$ fs$)$	$\eta(\Delta t = 0.5$ fs$)$	$\eta(\Delta t = 0.5$ fs$)$ (nonadiabatic)
0.999	2	0.51	0.31	0.56
0.9995	3	0.41	0.27	0.54
0.9999	4	0.50	0.42	0.60

time step. We find that with molecular dynamics time steps of 1 fs or 0.5 fs, the total energy is conserved[43] whenever $N_{states} \geqslant 10$. The energy is conserved fairly well with $N_{states} = 8$, but occasionally we saw large (~ 0.1 eV) and rapid (~ 50 fs) excursions in the total energy for this smaller basis. Large energy changes on such a fast time scale are a sign that the molecular dynamics is not correct (presumably, the two-electron ground state needs to mix in unavailable higher-lying single-electron states in order for the HF force to be consistent with the ground-state energy), so we reject $N_{states} = 8$ as too small. Taking $N_{states} = 10$ results in drift just barely acceptable by the standard mentioned above, but because of the $\sim N_{states}^4$ scaling in the size of the full CI matrix, we choose the smallest possible number of single-electron states, here $N_{states} = 10$, even though energy conservation does improve with $N_{states} = 12$.

Having determined that $N_{states} = 10$ suffices to maintain adequate energy conservation, we turn next to setting the parameters that make molecular dynamics practical, f_{imp}, and τ_{update}. We ran 1–2 ps ground-state trajectories for $f_{imp} = 0.999$, 0.9995, and 0.9999, and found that in order to avoid visible discontinuities (greater than ~ 0.05 eV) in the total energy at the update points, we must choose $\tau_{update} = 2$, 3, and 4 fs, respectively,[44] and either $\Delta t = 0.5$ fs or $\Delta t = 1$ fs. Using Eq. (15), we have tabulated the efficiency factor, η, for these parameters. The results, presented in Table IV, show that for ground-state adiabatic molecular dynamics runs the important-states scheme gives the greatest gain in computational efficiency with $f_{imp} = 0.9995$ and $\tau_{update} = 3$ fs. Likewise, Table IV shows that for nonadiabatic dynamics with $\Delta t = 0.5$ fs, taking $\tau_{update} = 3$ fs, $f_{imp} = 0.9995$ for the first excited state, and $f_{imp} = 0.99$ for the lowest other five two-electron states provides the best combination of efficiency and accuracy. We therefore choose $\Delta t = 0.5$, $\tau_{update} = 3$ fs, and $f_{imp} = 0.9995$ for both the singlet and triplet nonadiabatic runs discussed below.

B. Nonadiabatic relaxation of excited dielectrons

We now apply our real-space, CI method with the important-states approximation to the MF/SH molecular dynamics algorithm to simulate the nonadiabatic relaxation of hydrated dielectrons. We shall examine the relaxation of both
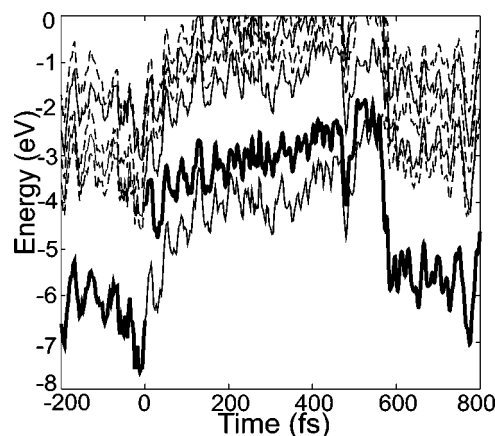

FIG. 1. Time dependence of the spin-singlet dielectron's adiabatic energy levels. The bold solid line indicates which state is occupied at any time. At time $t = 0$ fs, the dielectronic wave function is instantaneously changed from the ground state to the first excited state ($a_i \rightarrow \delta_{i2}$ in the notation of the Appendix). For clarity, we display every *other* two-electron eigenstate beginning with the second excited state and keep only the lowest nine adiabatic eigenstates (that is, only states 1, 2, 3, 5, 7, and 9 are shown).

spin-singlet and spin-triplet dielectrons following excitation from the equilibrium ground state to the first excited state. The initial configurations and water velocities used for the nonadiabatic runs were taken from long singlet and triplet ground-state trajectories that will be discussed in detail in a subsequent paper.[45]

Figure 1 shows the eigenenergy history for the nonadiabatic dynamics of a spin-singlet dielectron after excitation from the ground to the first excited state. Before excitation at $t = 0$, the singlet dielectron occupies a single, slightly aspherical (cf. Ref. 38 and Fig. 2) cavity; the dielectron charge density has a radius of gyration of about 2.4 Å, 20% larger than that for the hydrated electron.[25] The ground state of the dielectron has a lower energy (~ -6.0 eV) than that of two noninteracting electrons in a single-electron cavity ($\sim 2 \times -2.7$ eV $= -5.4$ eV).[25] This is surprising because the Coulomb and exchange interactions add ~ 4.5 eV to the ground-state energy of the singlet dielectron, which means that each electron has an extra ~ 2.5 eV favorable interaction with the solvent when in the dielectron cavity than in a single-electron cavity.[46] This extra stabilization leads to more bound single-electron states than the three seen for a single electron and, as we will show in a subsequent paper,[45] leads to an optical absorption spectrum with significant oscillator strength to the blue of the absorption of the single hydrated electron.

Upon excitation, we see in Fig. 1 the usual[8–11,14,15] rapid destabilization of the ground state as the solvent structure rearranges to accomodate the newly occupied excited state. After the Stokes shift has brought the ground and excited states close in energy, solvent motions induce a nonadiabatic transition back to the ground state, following which the ground state then rapidly reequilibrates. We can understand the driving force behind the dynamics both after excitation and after the nonadiabatic transition back to the ground state by examining the charge densities of the ground and first excited states following the initial excitation. Figure 2 shows

Ground | Excited

t = 0 fs

t = 150 fs
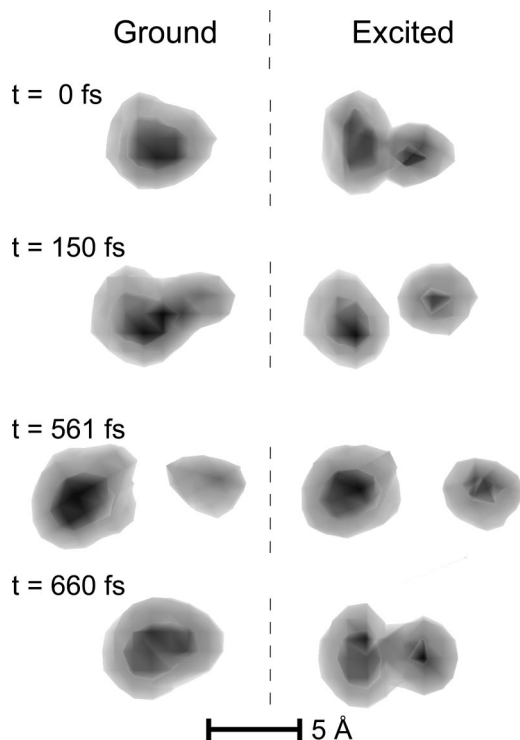
t = 561 fs

t = 660 fs

5 Å

FIG. 2. Three-dimensional contour plots of the dielectron charge density of the spin-singlet dielectron ground (left column) and first-excited (right column) states for the indicated times t after excitation. The lighter outer contours show the dielectron charge density at 10% of the maximum value, and the darker inner contours show the density at 50% of the maximum density. The nonadiabatic transition to the ground state occurs at the time $t = 561$ fs.
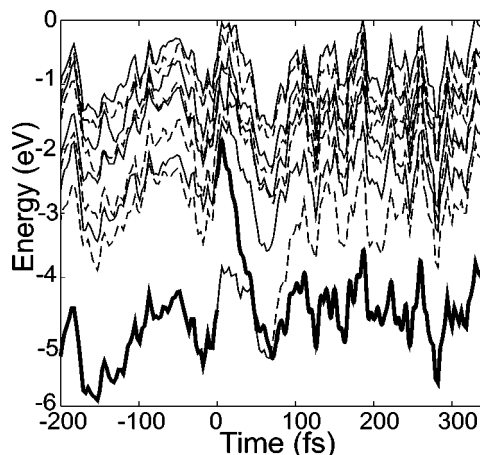

FIG. 3. Time dependence of the spin-triplet dielectron's adiabatic energy levels. The bold solid line indicates which state is occupied at any time. At time $t = 0$ fs, the dielectronic wave function is instantaneously changed from the ground state to the first excited state ($a_i \rightarrow \delta_{i2}$ in the notation of the Appendix). Only the lowest nine adiabatic eigenstates are shown.

that at time $t = 0$ fs (just before the excitation) the ground-state charge density is concentrated in a single, somewhat aspherical cavity. On excitation to the first excited state, the charge density acquires two lobes that are slightly offset from the ground state's center, but with most of the charge still contained in the original cavity.[47] In response to this change in the charge density the solvent moves to occupy the narrow waist of the excited-state charge density, driving up the energy of the ground state. After 150 fs, the lobes of the excited state have split into two holes separated by ~ 5.8 Å, and the unoccupied ground state has more charge in one of the holes, with some charge density spreading to the other hole.[48] A nonadiabatic transition back to the ground state takes place 561 fs after the excitation. The subsequent re-equilibration happens because the newly occupied ground state has most of its charge in only one of the holes, so the solvent can quickly squeeze out the nearly empty hole and repolarize around the occupied cavity to regenerate the equilibrated dielectron state.

Figure 3 shows the eigenenergy history for the nonadiabatic dynamics of a spin-triplet dielectron after excitation from the ground to the first excited state. Before excitation at $t = 0$, the triplet dielectron occupies a peanut-shaped cavity (cf. Ref. 38 and Fig. 4). In order to characterize this nonspherical state, we have calculated the principal moments of inertia of the triplet dielectron charge distribution (divided by the electron mass). The square roots of these moments give a measure of the size of the dielectron along the principal axes,

and their average values are 8.1 Å, 7.9 Å, and 2.6 Å; the almost-cylindrical symmetry of the triplet dielectron density is shown by the near equality of the two largest moments. The ground-state energy of the triplet dielectron (~ -4.7 eV) is *greater* than for two widely separated hydrated electrons ($\sim 2 \times -2.7$ eV $= -5.4$ eV),[25] implying that the triplet dielectron is at best metastable. The Coulomb (~ 4.3 eV) and exchange (~ -1.2 eV) interactions contribute a net ~ 3.1 eV to the triplet energy, indicating that the peanut-shaped cavity around the triplet dielectron provides ~ 1.2 eV more favorable electron-solvent interaction per electron than does a spherical single-electron cavity. Just as in the singlet case, this extra stabilization leads to more triplet bound states than the single electron has. However, as we will show in a subsequent paper,[45] the triplet dielectron has a smaller gap between the ground and excited states, resulting in less oscillator strength to the blue of the absorption spectrum of the single hydrated electron than for the singlet dielectron.

The mechanism and time scale for relaxation of the spin-triplet dielectron are very different than for the spin-singlet case. Figure 3 shows that excitation to the first adiabatic eigenstate leads to a very rapid reduction in the energy of the *excited* state, in contrast to the slower shift in ground-state energy for the spin-singlet case. Within about 50 fs, the Stokes shift causes the two lowest-lying eigenstates to become nearly degenerate, which lets the solvent quickly induce a nonadiabatic transition to the ground state. The triplet relaxation does resemble that of the singlet in that it requires a large Stokes shift before a nonadiabatic transition to the ground state can take place [cf. Eq. (A2)], but the rapid stabilization of the occupied excited state is the opposite of what is seen in the other examples of nonadiabatic dynamics in water.[8,9,11,14,15] The origin of this reversal can be seen in Fig. 4. Upon excitation to the excited state at time $t = 0$ fs, the region of highest charge density is transferred from each of the two lobes of a peanut-shaped ground state to the center of the cavity near the narrowest part of the ground-state

Ground   Excited

t = 0 fs

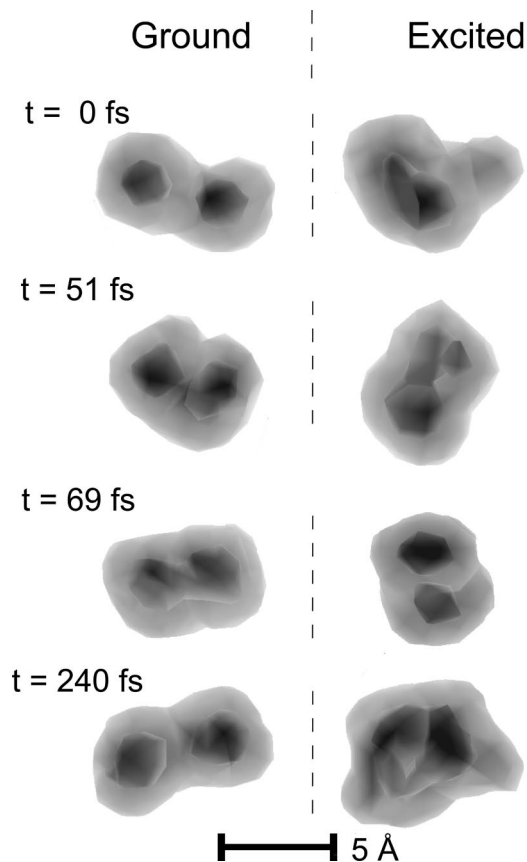t = 51 fs

t = 69 fs

t = 240 fs

5 Å

FIG. 4. Three-dimensional contour plots of the dielectron charge density of the spin-triplet dielectron ground (left column) and first-excited (right column) states for the indicated times t after excitation. The lighter outer contours show the dielectron charge density at 10% of the maximum value, and the darker inner contours show the density at 50% of the maximum density. The nonadiabatic transition to the ground state occurs at the time $t = 69$ fs.

charge density. The appearance of charge in a region previously occupied only by water molecules is accompanied by a large force repelling the now unfavorably solvating first-shell water molecules, and we speculate that motion of water out of this region is what drives the rapid solvent stabilization of the excited state. If this is indeed the case, then the spin-singlet and spin-triplet relaxations differ because in the singlet case excitation largely moves charge density from one place to another inside the original cavity, whereas the excitation of triplet dielectrons results in charge density inside the repulsive region of the water-electron pseudopotential. Figure 4 also shows that by time $t = 51$ fs, the ground- and excited-state charge densitites are (energetically nearly degenerate) perpendicular peanut shapes that are slightly more compact than the size of the equilibrium ground-state peanut. A few tens of femtosecond later, at $t = 69$ fs, a nonadiabatic transition takes place and within just a few hundred femtoseconds the triplet dielectron regains its equilibrium charge distribution, as is shown by Figs. 3 and 4.

The calculations presented here only scratch the surface of hydrated dielectron system. In forthcoming papers,[45] we will describe in detail the equilibrium properties of hydrated dielectrons, including discussions of their geometry, stability, spectroscopy, and nonequilibrium dynamics following pho-

toexcitation, with an emphasis on the role played by exchange in determining excited-state lifetimes and solvation dynamics.

V. DISCUSSION

In this paper we have introduced a method for calculating nonadiabatic mixed QM/CM dynamics for interacting electrons in disordered condensed-phase systems. Nonadiabatic dynamics requires not just the electronic ground-state density, but the full ground- and excited-state wave functions. We have shown that these many-electron wave functions can be computed by a novel real-space CI approach. In practice, the method relies on two new developments, one static and the other dynamical, to make multielectron nonadiabatic dynamics computationally feasible. First, we have introduced an efficient real-space quadrature to calculate the Coulomb and exchange interactions between electrons in a disordered system. This quadrature uses a low-order finite-element expansion of the electronic wave functions and works well even for single-electron wave functions that cannot be simply represented by Fourier (or other orthogonal eigenfunction) components. Second, we have introduced the idea of ''important states'' to improve the efficiency of nonadiabatic mixed QM/CM dynamics for multielectron systems. By periodically identifying those single-electron product basis states that contribute significantly to the many-electron eigenstates and constructing the CI matrix for just this sub-basis (between updates), we were able to reduce the cost of solving the multielectron quantum problem by nearly 50% with negligible error.

We combined our real-space/important-states CI method with the MF/SH (Ref. 21) algorithm for nonadiabatic QM/CM dynamics and studied the nonadiabatic relaxation dynamics of the hydrated dielectron. To the best of our knowledge, this is the first CI-based calculation of multielectron nonadiabatic solvation dynamics. We plan to study both the equilibrium and nonequilibrium properties of the hydrated dielectron in detail in future work,[45] but the limited results of Sec. IV were sufficient to demonstrate that the methods introduced here do allow the simulation of multielectron, condensed-phase, nonadiabatic dynamics. Work is also underway in our group to incorporate two-electron calculations into simulations of charge-transfer-to-solvent reactions (CTTS) in systems with solvated alkali metal anions.

We close with some comments on possible extensions to the methods introduced in this paper. In addition to the fixed-spin algorithm presented here, it would be straighforward to incorporate solvent-induced or external magnetic fields into the formalism in order to explore how intersystem crossings might affect many-electron dynamics and relaxation in the condensed phase. Finally, it is important to note that even though the examples considered in this paper had only two electrons, the algorithm presented here can be generalized to larger numbers of electrons. Certainly, any many-electron molecular dynamics calculation can make use of the idea of keeping only important states in an expansion basis, regardless of whether or not the basis states are of the CI product form. Furthermore, any CI treatment for more than two electrons will require the evaluation of Coulomb and exchange

integrals of the form of Eq. (12), so the real-space quadrature we have introduced can be used with more than two electrons *for no more computational cost* than with two electrons. Of course, at some point the cost of diagonalizing the many-electron CI matrix must become greater than the cost of computing the Coulomb and exchange integrals, but it will be interesting to discover just how far full, multireference CI can be taken in disordered systems.

ACKNOWLEDGMENTS

APPENDIX: MEAN-FIELD WITH SURFACE HOPPING FOR CI WAVE FUNCTIONS

The CI method we have developed produces multielectron wave functions for both the ground and excited states of any given electron–environment interaction. For example, given the positions at any instantaneous configuration of some solvent along with the electron-solvent interaction, we can find the (adiabatic) eigenstates Ψ_i for the multielectron system. Armed with these states, the system can be propagated using a variety of mixed quantum and classical schemes.[1] In this Appendix, we review the MF/SH algorithm introduced by Prezhdo and Rossky, and give explicit formulas for the Hellmann-Feynman force and nonadiabatic coupling for two-electron CI wave functions. For traditional surface hopping or adiabatic (Born-Oppenheimer) dynamics, the equations shown here apply with the appropriate (trivial) specialization.

The MF/SH algorithm combines MF dynamics, in which the state of the quantum subsystem is a normalized mixture of the adiabatic eigenstates, $|\Psi\rangle = \Sigma_i a_i(t)|\Psi_i\rangle$, with surface hopping, which allows discontinuous transitions between states. The classical MF forces on the solvent degrees of freedom are given by the HF force described below, and the adiabatic expansion coefficients a_i evolve according to the time-dependent Schrödinger equation

$$i\hbar \dot{a}_i = \sum_j a_j(t)\left(E_j \delta_{ij} - i\hbar\left\langle \Psi_j \left| \frac{\partial \Psi_i}{\partial t} \right.\right\rangle\right), \tag{A1}$$

where E_j is the adiabatic energy of the two-electron state j. The factor $\langle \Psi_j | \partial \Psi_i / \partial t \rangle$ is called the nonadiabatic coupling coefficient. Integrating Eq. (A1) and the classical equations of motion using the HF force ensures that the total energy of the mixed quantum/classical system is conserved.

The sorts of mixed states just described arise from passage through regions with strong nonadiabatic coupling; away from regions of strong nonadiabatic coupling, quantum systems (especially condensed-phase systems) are not typically found in mixed states. This implies that every so often the wave function is reset to a pure state; such reductions (or collapses) of the wave function are ascribed to decoherence. Decoherence is taken into account in MF/SH by inducing discontinuous changes in the MF wave function whenever a "mean-field consistency" criterion (described below) is violated. In addition, quantum transitions between adiabatic states, surface hops (SHs), are incorporated by allowing transitions between different adiabatic states.

In numerical implementations, the nonadiabatic coupling coefficients can be easily calculated using, e.g., a centered difference for the time derivative, which is all that is needed to propagate the wave function. To include surface hopping, however, it has proven convenient to write the nonadiabatic coupling in a form that highlights the coupling to nuclear degrees of freedom.[13] To do this, one simply expands the nonadiabatic coupling in terms of displacements of the classical degrees of freedom,

$$\left\langle \Psi_j \left| \frac{\partial}{\partial t} \Psi_i \right.\right\rangle = \dot{\mathbf{R}} \cdot \langle \Psi_j | \nabla_{\mathbf{R}} \Psi_i \rangle$$

$$= \dot{\mathbf{R}} \cdot \frac{\langle \Psi_j | \nabla_{\mathbf{R}} \hat{H} | \Psi_i \rangle}{(E_i - E_j)} \equiv \dot{\mathbf{R}} \cdot \mathbf{d}_{ij}(\mathbf{R}), \tag{A2}$$

where we have defined $\mathbf{d}_{ij}$, the *nonadiabatic coupling vector* between states i and j.[49] It is computationally most convenient to use the second-to-last expression above to compute $\mathbf{d}_{ij}$ because it can be calculated using the same code as for the Hellmann–Feynman forces [see Eq. (A3) below].[50] Note that in the absence of magnetic fields to mix the singlet and triplet ($\pm$) states, the nonadiabatic coupling between states with differing spin symmetry vanishes.[29]

For the mean-field trajectory, the HF force associated with each degree of freedom λ is

$$\mathbf{F}_\lambda = -\langle \Psi | \partial \hat{H} / \partial \lambda | \Psi \rangle$$

$$= -\sum_{i,j} a_i a_j^\star \sum_{n,m} \sum_{n',m'} c_{nm}^i c_{n'm'}^j$$

$$\times \int d\mathbf{r} \left(\frac{\partial H_1(\mathbf{r})}{\partial \lambda} \right) \rho^{(2)}_{n'm',nm}(\mathbf{r}), \tag{A3}$$

where we have taken advantage of the symmetry $\hat{H}_1 = \hat{H}_2$ and noted that $(\partial \hat{V}_{12}/\partial \lambda) = 0$.[51,52] This force has the same form as the single-electron HF force, except that a two-electron density $\rho^{(2)}(\mathbf{r})$ replaces the single-electron density as the effective classical charge density. The two-electron density $\rho^{(2)}(\mathbf{r})$ can in turn be written in terms of diagonal $[\rho^{(1)}_{aa}(\mathbf{r}) = |\psi_a(\mathbf{r})|^2]$ and off-diagonal $[\rho^{(1)}_{ab}(\mathbf{r}) = \psi_a(\mathbf{r})\psi_b^\star(\mathbf{r})]$ one-electron densities:

$$\rho^{(2)}_{nm,n'm'}(\mathbf{r}) = [\rho^{(1)}_{n'n}(\mathbf{r})\delta_{m'm} + \rho^{(1)}_{m'm}(\mathbf{r})\delta_{n'n}$$
$$\pm \rho^{(1)}_{m'n}(\mathbf{r})\delta_{n'm} \pm \rho^{(1)}_{n'm}(\mathbf{r})\delta_{nm'}],$$

$$\rho^{(2)}_{nn,n'm'}(\mathbf{r}) = \sqrt{2}[\rho^{(1)}_{n'n}(\mathbf{r})\delta_{m'n} + \rho^{(1)}_{m'n}(\mathbf{r})\delta_{n'n}],$$

$$\rho^{(2)}_{nn,n'n'}(\mathbf{r}) = 2\rho^{(1)}_{nn}(\mathbf{r})\delta_{nn'}. \tag{A4}$$

The plus signs are for spin-singlet states, the minus signs are for spin-triplet states, and the latter two equations only apply for the spin-singlet case.

As we have already pointed out, the MF/SH algorithm uses a reference trajectory to incorporate decoherence in an *ad hoc* manner. In ordinary MF dynamics, the state of the quantum subsystem is described by the expansion coefficients a_i, as noted above, but an additional piece of bookkeeping is used to include surface hopping in MF/SH dynamics; at each time, the system is considered to be "in" a particular adiabatic state (even though the true state is actually a mixture). The mean-field part of the algorithm then uses two distinct classical systems to include dephasing in an approximate way. The *physical* coordinates **R** are those of the actual classical system, whereas a second set of *reference* coordinates $\mathbf{R}_{ref}$ comprises a fictitious system which is used to decide when to collapse the mean-field wave function to the pure reference state n_{ref} by setting $a_j = \delta_{j,n_{ref}}$. The physical coordinates **R** obey mean-field dynamics, whereas the reference coordinates propagate according to forces determined by just the reference two-electron eigenstate, $|\Psi_{ref}\rangle = |n_{ref}\rangle$ associated with $\mathbf{R}_{ref}$, not **R**. The HF force for the reference trajectory can be calculated with Eq. (A3), with $a_i = \delta_{i,n_{ref}}$, and the charge densities determined using the single-electron states associated with $\mathbf{R}_{ref}$, as mentioned above.

Initially, the reference positions and velocities match the physical coordinates and velocities, but the reference trajectory evolves according to the reference HF forces described above instead of the MF forces from the mixed state. As more and more nonreference states begin to mix into the MF wave function, the physical and reference coordinates and momenta (denoted **P** and $\mathbf{P}_{ref}$) diverge. This divergence is used as a criterion for *MF rescaling*, which mimics decoherence by resetting the mixed state parameters $a_i \rightarrow \delta_{i,n_{ref}}$, $\mathbf{R}_{ref} \rightarrow \mathbf{R}$ and $\mathbf{P}_{ref} \rightarrow \mathbf{P}$ whenever the physical and reference trajectories violate the MF consistency criteria,

$$\frac{|\mathbf{P}^i - \mathbf{P}^i_{ref}|}{|\mathbf{P}^i + \mathbf{P}^i_{ref}|} \ll 1, \tag{A5}$$

$$|\mathbf{R}^i - \mathbf{R}^i_{ref}| \ll a_0, \tag{A6}$$

for any classical coordinate i. The specific limits on position and momentum deviation used to determine rescaling are free parameters in this theory and, as such, must be determined empirically for any given system. As these limits approach zero (i.e., if no mixing is allowed), the MF dynamics reduces to motion on a single Born–Oppenheimer potential energy surface (so-called adiabatic dynamics).

Surface hopping is incorporated into the MF/SH by introducing a second wave function which, following Wong and Rossky,[23] we call the *auxilliary* wave function $|\Psi_{aux}\rangle$. Note that our auxilliary wave function is called the *primary* wave function by Prezhdo and Rossky,[21] and our MF wave function is what Prezhdo and Rossky originally referred to as the auxilliary wave function. We reemphasize that here we use Wong and Rossky's convention.[23] The auxilliary wave function evolves in time according the same Schrödinger equation that governs the physical MF (mixed-state) evolution, Eq. (A1), but its expansion coefficients a_i^{aux} are never reset. For each time step in which no MF rescaling takes place, there is a possibility that the system will undergo a surface hop, in which the reference state n_{ref} changes to state j. Surface hops between states i and j occur stochastically, with a probability $P_{i \rightarrow j}$ given by Tully's fewest-switches prescription[22]

$$P_{i \rightarrow j} = -2Re\left(\frac{a_j^{aux}}{a_i^{aux}} \left\langle \Psi_j \left| \frac{\partial \Psi_i}{\partial t} \right\rangle \right) \Delta t, \tag{A7}$$

where Δt is the molecular dynamics time step and the above form is only valid when Ψ_i and Ψ_j are normalized *adiabatic* eigenstates. When a transition to state j occurs, the MF expansion coefficients change discontinuously to $a_i = \delta_{ij}$ and the reference trajectory changes to match the physical one, $\mathbf{R}_{ref} \rightarrow \mathbf{R}$ and $\mathbf{P}_{ref} \rightarrow \mathbf{P}$.

The final aspect of the MF/SH algorithm is the same as for other SH methods, and this is to ensure energy conservation following either a mean-field rescaling or a surface hop. Every time either a mean-field rescaling or a surface hop takes place, the energy in the quantum-mechanical subsystem changes discontinously by an amount ΔE_{QM}. To conserve the total energy in the system, therefore, any excess energy must be dumped into the classical degrees of freedom and any deficit must be taken from the classical kinetic energy. Each classical degree of freedom receives or donates energy according to how much it contributes to the nonadiabatic coupling, as determined by Eq. (A2). The details of this partitioning have been discussed elsewhere[13,21] and remain unchanged for the two-electron case.

[1] An overview of various mixed QM/CM methods can be found in *Classical and quantum dynamics in condensed phase simulations: proceedings of the International School of Physics "Computer simulation of rare events and dynamics of classical and quantum condensed-phase systems": Euroconference on "technical advances in particle-based computational material sciences,"* edited by B. J. Berne, G. Cicotti, and D. F. Coker (World Scientific, Singapore, 1998).
[2] O. V. Prezhdo, J. Chem. Phys. **117**, 2995 (2002).
[3] W. H. Miller, J. Phys. Chem. A **105**, 2942 (2001).
[4] E. J. Heller, J. Chem. Phys. **62**, 1544 (1975); **75**, 2923 (1981).
[5] G. D. Billing, Phys. Chem. Chem. Phys. **4**, 2865 (2002); Chem. Phys. Lett. **343**, 130 (2001); C. Coletti and G. D. Billing, *ibid.* **368**, 289 (2003).
[6] R. Car and M. Parrinello, Phys. Rev. Lett. **55**, 2471 (1985).
[7] M. Dahlbom, W. Beenken, V. Sundström, and T. Pullerits, Chem. Phys. Lett. **364**, 556 (2002).
[8] F. Webster, P. J. Rossky, and R. A. Friesner, Comput. Phys. Commun. **63**, 494 (1991).
[9] O. V. Prezhdo and P. J. Rossky, J. Phys. Chem. **100**, 17094 (1996).
[10] E. Neria, A. Nitzan, R. N. Barnett, and U. Landman, Phys. Rev. Lett. **67**, 1011 (1991).
[11] B. J. Schwartz and P. J. Rossky, J. Phys. Chem. **98**, 4489 (1994); **99**, 2953 (1995); J. Chem. Phys. **101**, 6902 (1994); **101**, 6917 (1994); Phys. Rev. Lett. **72**, 3282 (1994); J. Mol. Liq. **65–66**, 23 (1995); B. J. Schwartz, E. R. Bittner, O. V. Prezhdo, and P. J. Rossky, J. Chem. Phys. **104**, 5942 (1996).
[12] M. D. Hack, A. M. Wensmann, D. G. Truhlar, M. Ben-Nun, and T. J. Martinez, J. Chem. Phys. **115**, 1172 (2001).
[13] S. Hammes-Schiffer and J. C. Tully, J. Chem. Phys. **101**, 4657 (1994).
[14] W.-S. Sheu and P. J. Rossky, J. Phys. Chem. **100**, 1295 (1996).
[15] C. J. Smallwood, R. E. Larsen, W. B. Bosma, and B. J. Schwartz, J. Chem. Phys. (in press).
[16] A. Staib and D. Borgis, J. Chem. Phys. **103**, 2642 (1995).
[17] W. Stier and O. V. Prezhdo, J. Phys. Chem. B **106**, 8047 (2002).
[18] One notable exception to the single-electron trend is a recent semiempir-

ical CI calculation of photoreaction dynamics, by M. Persico, G. Granucci, S. Inglese, T. Laino, and A. Toniolo, J. Mol. Struct.: THEOCHEM **621**, 119 (2003).

[19] S. E. Bradforth and P. Jungwirth, J. Phys. Chem. A **106**, 1286 (2002).

[20] A. Szabo and N. S. Ostlund, *Modern Quantum Chemistry: Introduction to Advanced Electronic Structure Theory* (Dover, New York, 1989).

[21] O. V. Prezhdo and P. J. Rossky, J. Chem. Phys. **107**, 825 (1997).

[22] J. C. Tully, J. Chem. Phys. **93**, 1061 (1990).

[23] K. F. Wong and P. J. Rossky, J. Phys. Chem. A **105**, 2546 (2001); J. Chem. Phys. **116**, 8418 (2002); **116**, 8429 (2002).

[24] J. Schnitker and P. J. Rossky, J. Chem. Phys. **86**, 3462 (1987).

[25] P. J. Rossky and J. Schnitker, J. Phys. Chem. **92**, 4277 (1988).

[26] J. Schnitker, K. Motakabbir, P. J. Rossky, and R. Friesner, Phys. Rev. Lett. **60**, 456 (1988); D. Borgis and A. Staib, Chem. Phys. Lett. **230**, 405 (1994); D. Borgis and S. Bratos, J. Mol. Struct. **437**, 537 (1997); C. Nicolas, A. Boutin, B. Lévy, and D. Borgis, J. Chem. Phys. **118**, 9689 (2003).

[27] An overview of the configuration interaction method can be found in Chap. 4 of Ref. 20

[28] $\hat{H}_1$ should be considered to mean $\hat{H}_1 \times \hat{I}_2$ in a direct product Hilbert space, where $\hat{I}$ is the identity operator, and similarly for $\hat{H}_2$. $\hat{V}_{12}$ cannot, of course, be represented as a direct product of single-electron operators: interactions between the electrons will not be diagonal in a one-electron basis.

[29] Because the Coulomb interaction does not affect the spin of an electron, spin flips can only be induced by terms in the electron-solvent Hamiltonians (e.g., by magnetic fields induced by moving charges in the solvent) or by direct spin-spin interactions. In this work, we will neglect such spin interactions, but we note that the extension to such cases is straightforward.

[30] D. Finocchiaro, M. Pellegrini, and P. Bientinesi, J. Comput. Phys. **146**, 707 (1998).

[31] The factor of 1/6 in the number of pairs of cubes that have distinct values of ϕ_{ij} results from the symmetry of the cubic lattice.

[32] For instance $\phi_{0,15}$ (that is ϕ between two cubes separated in the x, y, or z direction by 15 steps should be about $1/15 = 0.0\overline{6}$. The tabulated value from our numerical computation is $\phi_{0,15} = 0.066666628...$, a difference of roughly 3×10^{-8}. To order 10^{-8}, therefore, we can use our tabulated values to compute ϕ between cubes within 16 grid points of each other, approximating all other values of ϕ by $1/r$.

[33] A. Alavi, J. Chem. Phys. **113**, 7735 (2000).

[34] M. P. Allen and D. J. Tildesley, *Computer Simulation of Liquids* (Oxford University Press, London, 1992).

[35] N. Basco, G. A. Kenney, and D. C. Walker, Chem. Commun. 917 (1969); N. Basco, G. A. Kenney-Wallace, S. K. Vidyarthi, and D. C. Walker, Can. J. Chem. **50**, 2059 (1972); D. Meisel, G. Czapski, M. S. Matheson, and W. A. Mulac, Int. J. Radiat. Phys. Chem. **7**, 233 (1975).

[36] K. J. Schmidt and D. M. Bartels, Chem. Phys. **190**, 145 (1995).

[37] See D. F. Feng, K. Fueki, and L. Kevan, J. Chem. Phys. **58**, 3281 (1978), and references therein.

[38] H.-P. Kaukonen, R. N. Barnett, and U. Landman, J. Chem. Phys. **97**, 1365 (1992).

[39] Z. H. Deng, G. J. Martyna, and M. L. Klein, Phys. Rev. Lett. **68**, 2496 (1992); **71**, 267 (1993); J. Chem. Phys. **100**, 7590 (1994); G. J. Martyna, Z. H. Deng, and M. L. Klein, *ibid.* **98**, 555 (1993).

[40] K. Toukan and A. Rahman, Phys. Rev. B **31**, 2643 (1985).

[41] F. Webster, E. T. Wang, P. J. Rossky, and R. A. Friesner, J. Chem. Phys. **100**, 4835 (1994).

[42] J. J. Sakurai, *Modern Quantum Mechanics*, revised ed. (Addison-Wesley, Reading, MA, 1994), Chap. 2.

[43] We define energy conservation by requiring any long-term drift in the total energy to be within the rms fluctuation over the course of a 2 ps run. The rms energy fluctuation is 0.08 eV for $\Delta t = 1.0$ and 0.02 eV for $\Delta t = 0.5$ fs.

[44] In the test run for $f_{imp} = 0.9999$, a single discontinuity was seen with $\tau_{update} = 4$ fs and not with $\tau_{update} = 3$ fs, so the $\tau_{update} = 4$ fs criterion is actually overly generous.

[45] R. E. Larsen and B. J. Schwartz (unpublished).

[46] A simple uncertainty-principle argument shows that the kinetic energy reduction associated with going from a cavity 4.0 Å in diameter to one 4.8 Å in diameter is less than ~ 0.1 eV.

[47] This change of shape from an "s-like" symmetry to a "p-like" symmetry is similar to what happens when a single hydrated electron is excited (see Refs. 9, 11, and 23), so it is not suprising that the time scale and mechanism of the Stokes shift are similar for the hydrated electron and the singlet dielectron.

[48] The two cavities of the excited state dielectron cannot properly be thought of as two separated single electrons because the exchange energy of ~ 0.5 eV indicates that each one-electron basis state has amplitude in both holes.

[49] Although Eq. (A3) is the most computationally efficient way to calculate the nonadiabatic coupling vector, some insight can be gained by expanding the two-electron wave functions, Ψ in terms of the product states. This expansion shows that the nonadiabatic coupling comes from a sum of direct coupling between the individual product states ($\sim c_{n'm'}^j c_{nm\pm}^i \langle n'm' | \nabla_{\mathbf{R}} | nm \rangle_{\pm}$) and coupling caused by changes in the CI expansion coefficients ($\sim c_{nm}^j \dot{c}_{nm}^i$). At first glance, the latter term appears quite similar to the Pulay force (Ref. 51) that corrects the Hellmann-Feynman force when the basis functions used to describe the quantum system vary with, e.g., nuclear postion. A difference between the adiabatic and nonadiabatic cases, however, is that this nonadiabatic "Pulay-type" term comes from changes in the adiabatic expansion coefficients rather than from changes in the basis. Unlike the Pulay force, therefore, the time dependence of the CI expansion coefficients is physically meaningful, and does not vanish in the limit that the basis set (here $|nm\rangle_{\pm}$) is complete.

[50] The step from the second to the third expression in Eq. (A2) is accomplished by noting that (Ref. 13) $\nabla_{\mathbf{R}}(\langle \Psi_j | \hat{H} | \Psi_i \rangle) = 0$, applying the product rule for derivatives and integrating by parts once.

[51] P. Pulay, in *Applications of Electronic Structure Theory*, edited by H. F. Schaefer III (Plenum, New York, 1977); M. Di Ventra and S. T. Pantelides, Phys. Rev. B **61**, 16207 (2000).

[52] One difference between the usual single-electron force and that for our CI case is that the CI expansion coefficients change in time. This change gives rise to a correction to the HF force, the Pulay force, Ref. 51, whenever a *finite* CI basis set is used (as will always be the case in practice). The specific form of the Pulay force for CI wave functions is straightforward, though tedious, to derive using first-order perturbation theory and the approach of Di Ventra and Pantelides (Ref. 51). We have examined the Pulay force for the hydrated dielectron system discussed in Sec. IV and found it to be negligible in comparison to the HF forces themselves, so we do not bother to explicitly display it here.

[53] C. C. Huang, G. S. Couch, E. F. Pettersen, and T. E. Ferrin, in Proceedings of the Pacific Symposium on Biocomputing, 1996, Vol. 1, p. 724. The CHIMERA code is freely available on the worldwide web at http://www.cgl.ucsf.edu/chimera